BBA - Biomembranes 1861 (2019) 1049–1056

Contents lists available at ScienceDirect

BBA - Biomembranes

journal homepage: www.elsevier.com/locate/bbamem

In vitro antileishmanial and cytotoxic activities of nerolidol are associated with changes in plasma membrane dynamics

Lais Alonso[a,b], Kelly Souza Fernandes[c], Sebastião Antônio Mendanha[a], Pablo José Gonçalves[a], Rodrigo Saar Gomes[d], Miriam Leandro Dorta[d], Antonio Alonso[a,*]

[a] Instituto de Física, Universidade Federal de Goiás, Goiânia, GO, Brazil
[b] Departamento de Farmácia e Farmacologia, Universidade Estadual de Maringá, Maringá, PR, Brazil
[c] Instituto Federal Goiano, Trindade, GO, Brazil
[d] Instituto de Patologia Tropical e Saúde Publica, Departamento de Imunologia e Patologia Geral, Universidade Federal de Goiás, Goiânia, GO, Brazil

ARTICLE INFO

Keywords:
Nerolidol
Leishmania
Macrophages
Membrane fluidity

ABSTRACT

The sesquiterpene nerolidol is a membrane-active compound that has demonstrated antitumor, antibacterial, antifungal and antiparasitic activities. In this study, we used electron paramagnetic resonance (EPR) spectroscopy and biophysical parameters determined *via* cell culture assays to study the mechanisms underlying the *in vitro* antileishmanial activity of nerolidol. The EPR spectra of a spin-labeled stearic acid indicated notable interactions of nerolidol with the cell membrane of *Leishmania amazonensis* amastigotes. The nerolidol IC_{50} values in *L. amazonensis* amastigotes and promastigotes were found to depend on the cell concentration used in the assay. This dependence was described by an equation that considers various cell suspension parameters, such as the 50% inhibitory concentrations of nerolidol in the cell membrane (c_{m50}) and the aqueous phase (c_{w50}) and the membrane-water partition coefficient of nerolidol ($K_{M/W}$). *Via* cytotoxicity (CC_{50}) and hemolytic potential (HC_{50}) data, these parameters were also determined for nerolidol in macrophages and erythrocytes. With a c_{w50} of 125 μM, macrophages were less sensitive to nerolidol than amastigotes and promastigotes, which had mean c_{w50} values of 56 and 74 μM, respectively. The estimated c_{m50} values of nerolidol for amastigotes and promastigotes and macrophages were between 2.6 and 3.0 M, indicating substantial accumulation of nerolidol in the cell membrane. In addition, the spin-label EPR data indicated that membrane dynamic changes occurred in *L. amazonensis* amastigotes at concentrations similar to the nerolidol IC_{50} value.

1. Introduction

Cutaneous leishmaniasis is the most common form of leishmaniasis, and over two-thirds of the new cases in 2015 occurred in 6 countries: Afghanistan, Algeria, Brazil, Colombia, Iran (Islamic Republic of) and the Syrian Arab Republic; moreover, it is estimated that between 600,000 and 1 million new cases occur annually worldwide [1]. The treatment options are pentavalent antimonials, amphotericin B deoxycholate, lipid formulations of amphotericin B, paromomycin, pentamidine isethionate and miltefosine; however, all of these medications have strong side effects [2].

Nerolidol is an aliphatic sesquiterpene alcohol that is present in the essential oils of many plants; thus, it is common in the human diet and has been approved by the U.S. Food and Drug Administration as a food flavoring agent. A recent report [3] indicated that nerolidol exhibits *in vitro* activity against cancer cells [4], bacteria [5], fungi [6,7] and Trypanosoma [8], *Leishmania* [9], Malaria [10,11] and *Babesia* [12] parasites. Nerolidol has been shown to increase the lipid fluidity in the stratum corneum, the most superficial layer of the skin [13,14], and the lipid fluidity in fibroblast membranes [15] as well as membrane models [16]. Nerolidol is considered an effective skin permeation enhancer with the ability to increase percutaneous permeation *in vitro* of the drugs nicardipine hydrochloride, hydrocortisone, carbamazepine and tamoxifen [17] as well as diclofenac sodium [18].

A recent report demonstrated that the half maximal inhibitory concentration (IC_{50}) of hydrophobic molecules, such as nerolidol [19] and miltefosine [20], in *Leishmania* (*Leishmania*) *amazonensis* culture is dependent on the cell concentration that is used in the assay. The equation describing this behavior involves the membrane-water partition coefficient of the drug ($K_{M/W}$) and the drug concentrations that inhibit 50% of the growth in the aqueous (c_{w50}) and membrane (c_{m50}) phases. Importantly, these biophysical parameters obtained from the fit

* Corresponding author.
E-mail address: alonso@ufg.br (A. Alonso).

https://doi.org/10.1016/j.bbamem.2019.03.006
Received 29 November 2018; Received in revised form 13 March 2019; Accepted 14 March 2019
Available online 16 March 2019
0005-2736/

of this equation to the experimental data do not depend on the cell concentration used in the experiment and allow a more comprehensive analysis of the mechanisms of action of the drug [20]. Although the mode of action of nerolidol is not yet well established, the mode of action of miltefosine is associated with membrane-lipids interactions, cytochrome *c* oxidase inhibition and apoptosis-like cell death [21]. This equation indicates that the drug IC_{50} values increase with the cell concentration only until reaching the value necessary to achieve the critical drug concentration in the membrane (c_{m50}) that decreases the parasite population by 50%. This type of behavior was also observed in an erythrocyte suspension by analyzing the miltefosine concentration necessary for 50% hemolysis at different cell concentrations. In this case, a c_{m50} of 111 mM was found, which is the miltefosine concentration in the erythrocyte membrane that causes 50% hemolysis [22].

Electron paramagnetic resonance (EPR) spectroscopy has been used to show that terpenes at concentrations near their IC_{50} values cause marked increases in the plasma membrane fluidity of *L.* (*L.*) *amazonensis* promastigotes [19]. Furthermore, the terpenes nerolidol, (+)-limonene, α-terpineol and 1,8-cineole at concentrations close to their IC_{50} values caused cell lysis of 4 to 9%, and this percentage was approximately 50% for terpene concentrations that were double or triple the IC_{50} values [19]. Scanning electron microscopy (SEM) of *L.* (*Viannia*) *braziliensis* promastigotes showed that nerolidol treatment at double the IC_{50} concentration caused shrinkage and roundness of the parasite cell body after 24 h [23]. In addition, the cytotoxicity of seven monoterpenes and nerolidol in cultured fibroblast cells showed a correlation with the concentrations of terpenes causing 50% hemolysis [20].

In this study, EPR spectroscopy was used to evaluate the interaction of nerolidol with *Leishmania* amastigote membranes at low cell concentrations to determine whether nerolidol concentrations that alter the parasite membrane are in the range of the usual inhibitory growth concentrations, such as 60 µM. The hemolytic potential of nerolidol was assessed for RBC in PBS and directly assessed using whole blood. In addition, the biophysical parameters c_{m50}, c_{w50} and $K_{M/W}$ for nerolidol in *L.* (*L.*) *amazonensis* promastigotes and amastigotes, mouse macrophages and human erythrocytes were assessed for comparison with the data reported for miltefosine to obtain a more comprehensive understanding of the mechanisms underlying the antiparasitic activities of these two compounds.

2. Materials and methods

2.1. Chemicals

Grace's insect medium, RPMI-1640 medium, L-glutamine, penicillin, streptomycin, 3-(4,5-dimethylthiazol-2-yl)-2,5-diphenyl tetrazolium bromide (MTT), sodium bicarbonate, nerolidol (98% purity, a mixture of cis and trans nerolidol, MW = 222.37 g/mol, CAS Number 7212-44-4) (Fig. 1) and 5-doxyl-stearic acid (5-DSA) (Fig. 1) were purchased from Sigma-Aldrich (St. Louis, MO, USA). Miltefosine was purchased from Avanti Polar Lipids Inc. (Alabaster, AL, USA).

2.2. Cells

Promastigotes and amastigotes of *L.* (*L.*) *amazonensis* (MHOM/BR/75/Josefa) reference strains were grown in 24-well microtiter plates containing 2 mL of Grace's insect medium supplemented with 20% FCS, 2 mM L-glutamine, 100 U/mL penicillin and 100 µg/mL streptomycin as previously described [24]. As reported, axenic *L.* (*L.*) *amazonensis* has been used because its morphology, structure and infectivity are similar to those of intracellular amastigotes and inconsistent with those of promastigotes [25–27]. Compared to the *in vitro* process used to obtain parasites directly from lesions, this method can provide higher concentrations of amastigotes and eliminate possible contamination by

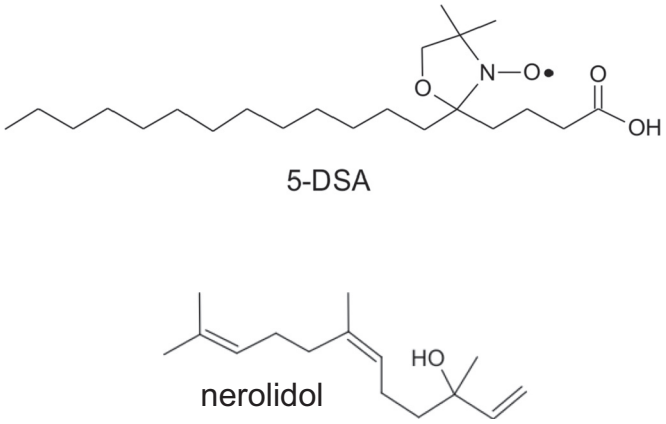

Fig. 1. Chemical structures. Nerolidol (represented in its cis isomer) and the spin label 5-DSA used in this study.

elements of vertebrate hosts. The tests were performed once these parasites reached the logarithmic phase of growth (6th day). The J774.A1 murine macrophage cell line was obtained from the cell bank of Rio de Janeiro (NCE/UFRJ). Cells were maintained in RPMI-1640 medium supplemented with 10% FCS, 2 mM L-glutamine, 100 U/mL penicillin and 100 µg/mL streptomycin at 37 °C in a humidified incubator containing 5% CO_2.

2.3. In vitro assays of antiproliferative activity and cytotoxicity in macrophages

Parasites or macrophages at several cell concentrations were treated with increasing concentrations of nerolidol (Fig. 1), which were initially diluted three times in ethanol and then diluted in culture medium supplemented with 10% FCS. The samples were incubated for 24 h in 96-well culture dishes (100 µL for parasites and 200 µL for macrophages) at 26 °C for promastigotes, 32 °C for amastigotes and 37 °C for macrophages in the presence of 8 different concentrations of nerolidol. Cell viability was assessed based on the reduction of MTT to formazan by mitochondrial reductases. The mean percentage of viable cells relative to the control was calculated for each nerolidol concentration, and the IC_{50} was then determined by fitting the concentration response to a sigmoid curve.

2.4. J774.A1 macrophage infection

J774.A1 cells were cultured in RPMI 1640 medium supplemented with 10% FCS, 2 mM L-glutamine, 11 mM sodium bicarbonate, 100 U/mL penicillin and 100 µg/mL streptomycin. Then, 4×10^6 cells/mL were infected for 3 h with GFP-transfected *L. amazonensis* (IFLA/BR/67/PH8; 5 parasites:1 cell) on the 6th day of growth. GFP (green fluorescent protein)-transfected *L. amazonensis* promastigotes were cultivated *in vitro* in Grace's insect medium supplemented as described above. Frequently, the GFP parasites were selected with 30 µg/mL Hygromycin B [28].

After 3 h of infection, the cells were washed with 1× PBS for the removal of non-internalized parasites and cultured for an additional 24 h in the presence of nerolidol at different concentrations and ethanol as control. Miltefosine was used as a control. The cells were then collected and analyzed by flow cytometry using a BD Accuri™ C6 Flow cytometry system (BD Bioscience, San Jose, CA, USA). The data were analyzed using FlowJo software (Tree Star, Ashland, OR, USA). Macrophages were selected by forward scatter *versus* side scatter (FSC *vs* SSC), and the percentage of cells expressing GFP+ was evaluated.

2.5. Hemolytic potential of nerolidol

Blood was donated by laboratory researchers and placed into EDTA-coated blood collection tubes under vacuum. One volume of blood was diluted in three volumes of PBS and centrifuged at 800 ×*g* for 10 min at 4 °C. The plasma and white blood cells were removed by aspiration, and the pellet was resuspended in PBS. This washing procedure was repeated three times. Hemolytic tests with nerolidol were performed with five concentrations of erythrocytes: 1.11, 5.55, 11.11, 22.22 and 55.55 × 10^8 cells/mM. To calculate the cell concentration in the suspension, a volume of 90 fL was considered for the erythrocytes. Nerolidol was initially diluted three times in ethanol and then in PBS containing ethanol to a final ethanol concentration of 5% (v/v); further dilutions were performed in PBS with 5% ethanol. For each erythrocyte concentration, 100 µL volume samples containing different concentrations of nerolidol were prepared and incubated for 2 h at 36.5 ± 1 °C. After incubation, 1.4 mL of PBS was added to each tube, and the samples were centrifuged again. The percentage of hemolysis was determined based on the absorbance of hemoglobin in the supernatant at 540 nm. The nerolidol concentration that caused 50% hemolysis (HC_{50}) was then determined by fitting the concentration response to a sigmoid curve.

To measure the hemolytic potential of nerolidol in whole blood, the plasma was separated by centrifugation at 2000 ×*g* for 10 min at 4 °C, and 10 samples of 58 µL of plasma containing nerolidol at different concentrations were prepared. Then, 42 µL of erythrocytes at 100% hematocrit was added to each sample to reconstitute total blood. The samples were incubated for 24 h at 7 ± 1 °C, and during this period, the samples were gently stirred several times. Hemolysis percentages were determined as described above.

2.6. Spin labeling and EPR spectroscopy

Amastigotes of *L.* (*L.*) *amazonensis* in suspension at 4 × 10^7 parasites/mL (2 mL) were incubated in culture medium without FCS for 2 h at 32 °C in the presence of eight nerolidol concentrations. After incubation, each sample was centrifuged at 1800 ×*g* for 10 min to increase the cell concentration to 8 × 10^7 parasites/mL and decrease the final volume to 50 µL. Then, the lipid spin label 5-DSA (Fig. 1) was incorporated into the *Leishmania* membranes. To label the membrane, a spin-label film was first prepared on the bottom of a test glass tube using a 1 µL aliquot of a 5-DSA ethanolic solution (4 mg/mL); after evaporation of the solvent, the samples containing 50 µL of amastigotes were added to the spin-label film and gently agitated. For the EPR measurements, each sample was transferred to a 1-mm-i.d. capillary tube, which was sealed using a flame.

A Bruker EMX Plus spectrometer (Rheinstetten, Germany) equipped with an ER4102ST cavity was used to perform the EPR measurements. Spectra were acquired using the following instrument settings: microwave power, 2 mW; modulation frequency, 100 kHz; modulation amplitude, 1.0 G; magnetic field scan, 100 G; sweep time, 168 s; and sample temperature, 25 °C. The best-fit EPR spectra were obtained using the nonlinear least-squares (NLLS) software developed by Freed JH and coworkers [29]. As in other studies [30,31], the motion parameter τ_c, *i.e.*, the rotational correlation time, was calculated using the following equation:

$$\tau_c = \frac{1}{6Rbar}, \quad (1)$$

where R_{bar} represents the rate of rotational Brownian diffusion and was given as an output from the NLLS program after the best-fit process. In this study, the best-fit spectra were calculated using a two-spectral-component model. The principal values of the g- and A-tensors were optimized and fixed in the simulations of all spectra. The values used for components 1 and 2 were as follows: g_{xx} (1) = 2.0080, g_{yy} (1) = 2.0060, g_{zz} (1) = 2.0017, A_{xx} (1) = 6.5 G, A_{yy} (1) = 6.2 G, A_{zz} (1) = 33.1 G, g_{xx} (2) = 2.0082, g_{yy} (2) = 2.0062, g_{zz} (2) = 2.0027, A_{xx} (2) = 5.7 G, A_{yy} (2) = 5.6 G and A_{zz} (2) = 31.2 G.

The average value of the motion parameter τ_C was calculated from parameters generated by the simulations using the following equation [32]:

$$\tau_C = f_1\tau_{C1} + f_2\tau_{C2}, \quad (2)$$

where f_1 and f_2 represent the relative fractions of the spin label in the less (1) and more (2) mobile components, respectively; and τ_{C1} and τ_{C2} are the respective rotational correlation times.

2.7. Statistical analysis

All data are presented as the mean ± S.D. of at least three independent experiments. The means were compared through a one-way analysis of variance (ANOVA). Tukey's test was used to identify significant differences ($P < 0.05$) between means among the different treatments.

3. Results

3.1. Growth inhibitory and cytotoxic nerolidol concentrations are dependent on the cell concentration used in the assay

The nerolidol IC_{50} values measured for promastigotes and amastigotes of *L. amazonensis* were dependent on the cell concentration used in the experiment (Fig. 2). Additionally, the nerolidol CC_{50} values measured in the J774.A1 murine macrophage cell line exhibited a cell concentration-dependent behavior (Fig. 3). Notably, for *L. amazonensis* promastigotes, the IC_{50} values ranged from ~80 µM when an initial cell concentration of 5 × 10^6 parasites/mL was used in the assay to > 1 mM when the test was started with 1 × 10^9 parasites/mL (Fig. 2). Significant variations in CC_{50} values were also observed when the concentration of macrophages in the assay was increased 20-fold (Fig. 3).

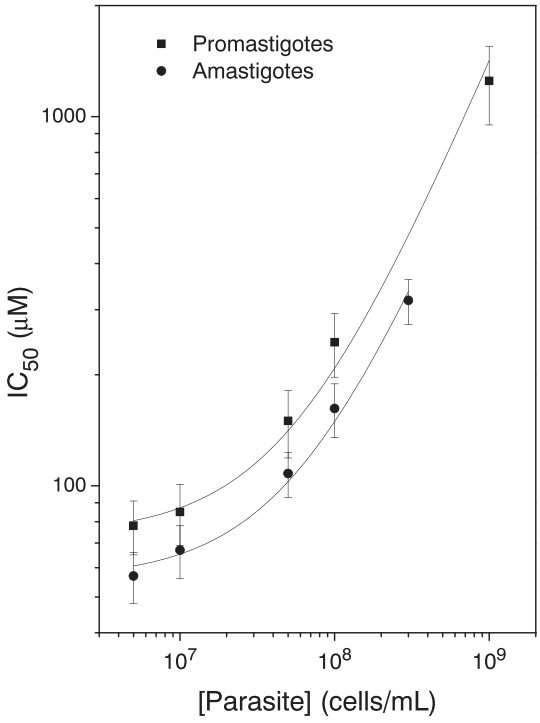

Fig. 2. IC_{50} values of nerolidol with *Leishmania amazonensis* amastigotes and promastigotes at several cell concentrations used at the beginning of the experiment. The best-fit curves presented for the amastigotes and promastigotes data are based on Eq. (6).

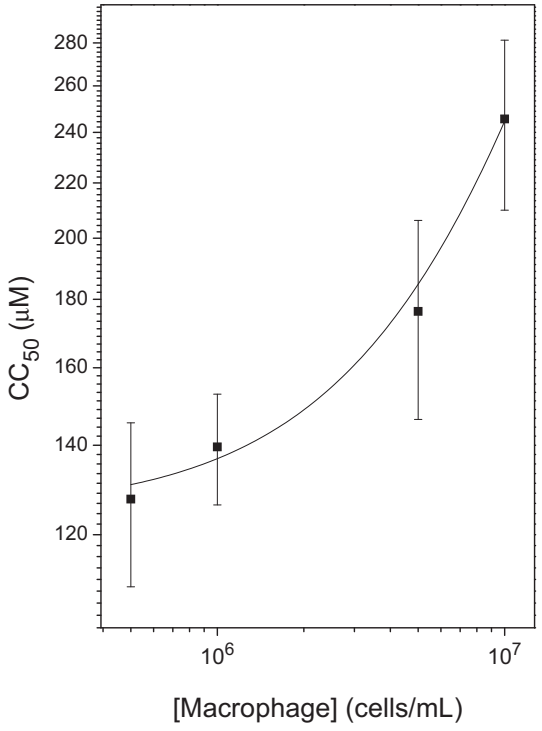

Fig. 3. CC_{50} values of nerolidol in the J774.A1 murine macrophage cell line for several cell concentrations used to start the assay. The best-fit curve shown is based on Eq. (6).

This type of behavior is generally observed for hydrophobic drugs that accumulate in the cell membrane and when the response in cell population reduction is associated with a critical concentration of the drug in the cell membrane. In previous works [20], the equation describing this behavior was presented, and it includes important cell suspension parameters, such as the membrane-water partition coefficient ($K_{M/W}$), which can be determined by fitting the parameters of this equation to the experimental data as shown in Figs. 1 and 2. The derivation of this equation can be understood as follows.

Consider a cell suspension with n_w moles of the test molecule in aqueous medium and n_m moles in the cell membrane. The molar concentration in the cell suspension (c_{sus}) can be calculated as follows:

$$c_{sus} = \frac{n_w + n_m}{V_w + V_m}, \tag{3}$$

where V_w is the volume of aqueous medium and V_m is the membrane volume of the cells in the suspension. Introduction of the molar concentration in the membrane (c_m) and in the aqueous phase (c_w) as well as the cell membrane-water partition coefficient $K_{M/W}$ ($K_{M/W} = c_m / c_w$) to Eq. (3) yields the following:

$$c_{sus} = \frac{c_w V_w + K_{M/W}\, c_w V_m}{V_w + V_m} \tag{4}$$

or

$$c_{sus} = \left[\frac{(V_w/V_m) + K_{M/W}}{(V_w/V_m) + 1}\right] c_w. \tag{5}$$

The value of the term in brackets approaches 1 for well-diluted samples ($V_w \gg V_m$) or for hydrophilic drugs (low $K_{M/W}$ values). In these cases, $c_{sus} = c_w$. However, for hydrophobic molecules and higher cell concentrations, the suspension can no longer be considered homogeneous and c_{sus} can be quite different from c_w.

The plasma membrane volume (V_{mc}) of each cell studied was estimated previously [20] from the cellular volume measured *via* optical microscope images. The estimated V_{mc} for amastigotes and promastigotes of *L. amazonensis* and rat macrophages were 2.98, 8.17 and 41.4 × 10^{-13} mL, respectively [20]. The volume of membrane inside the cell was neglected due to a lack of reliable data. In a 1-mL suspension, V_m is equal to V_{mc} multiplied by the number of cells per mL (c_c). V_w is approximately equal to 1 mL, the total volume of the suspension, because the value of V_m is very small ($< 1 \times 10^{-3}$ mL). Therefore, substituting V_w / V_m with $(V_{mc} \cdot c_c)^{-1}$, we can rewrite Eq. (5) as follows:

$$c_{sus} = \left[\frac{(V_m \bullet c_c)^{-1} + K_{M/W}}{(V_m \bullet c_c)^{-1} + 1}\right] c_w. \tag{6}$$

Notably, the IC_{50} (Fig. 2) and CC_{50} (Fig. 3) data correspond to the c_{sus} values in Eq. (6), and in these cases, the values of c_w can be considered equivalent to c_{w50} because these values represent the nerolidol concentration in the aqueous phase of the cell suspension that resulted in a 50% cell population decrease. In addition, the c_{m50} value calculated using $K_{M/W} = c_{m50} / c_{w50}$ is the critical concentration in the cell membrane that decreases the cell population by 50%. Compared with IC_{50}, the c_{w50} and c_{m50} values are independent of the cell concentration used in the assay, and this fact demonstrates that these cell suspension parameters are more suitable for comparing the effects of a drug on different cell types. It should be mentioned that the volume of the membrane inside the cell was neglected; thus, if this value is equal to the plasma membrane volume, then the values of $K_{M/W}$ and c_{m50} would fall by half.

3.2. Hemolytic potential of nerolidol in PBS with 5% ethanol (v/v) and whole blood

The concentration of nerolidol that produces 50% hemolysis (HC_{50}) is also affected by the erythrocyte concentration used in the assay, and the experimental data shown in Fig. 4 also exhibit the behavior described by Eq. (6). Reducing the erythrocyte concentration in the suspension by 50-fold caused the nerolidol HC_{50} to decrease from approximately 2300 to 300 μM. It is important to mention the

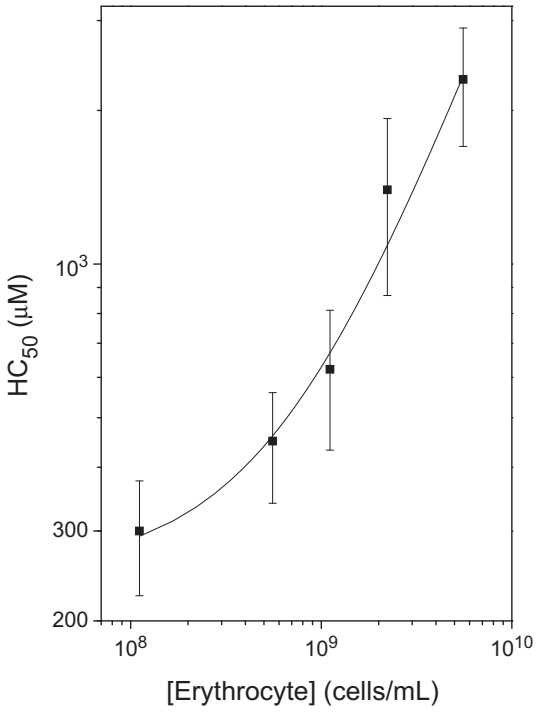

Fig. 4. Experimental data and a theoretical curve calculated using Eq. (6) (see text for details) for the nerolidol concentration that produces 50% hemolysis (HC_{50}) *versus* the erythrocyte concentration used in the experiment.

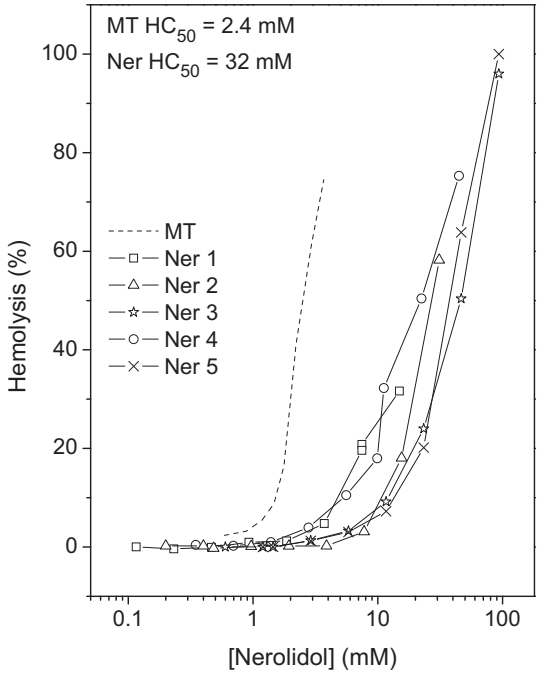

Fig. 5. Hemolysis curve for nerolidol incubated in whole blood for 24 h at 7 ± 1 °C. The nerolidol data points are from five independent experiments. The curve obtained for miltefosine in previous work is shown for comparison [22]. The estimated nerolidol concentration required for 50% hemolysis (HC_{50}) is indicated.

experimental difficulties encountered in performing the hemolysis experiments using nerolidol diluted in PBS. The experimental results were more reproducible and reliable when nerolidol was initially diluted in ethanol, and a final concentration of 5% ethanol was maintained in the experiments.

Fig. 5 shows the hemolysis curve of nerolidol in whole blood compared with the curve for miltefosine under similar conditions [22]. Nerolidol was added to plasma, and red blood cells were then added to the plasma to reconstitute whole blood. The nerolidol and miltefosine concentrations in whole blood that resulted in 50% hemolysis were 2.4 and 32 mM, respectively.

3.3. Best-fit parameters obtained from fittings using Eq. (6)

The parameters $K_{M/W}$, c_{w50} and c_{w50} obtained from the fitting of the curves shown in Figs. 1, 2 and 3 are presented in Table 1. The data for miltefosine reported in a previous work [20] are also shown for comparison. The $K_{M/W}$ values indicated that the affinity of nerolidol for *Leishmania* and macrophage membranes were markedly higher than the affinity for the erythrocyte membrane, whereas in miltefosine, the differences in $K_{M/W}$ values for these three types of cells were not as pronounced. On the other hand, the critical concentration that causes disruption in the erythrocyte membrane (c_{m50} = 0.3 M) was also markedly lower than that in *Leishmania* (c_{m50} = 2.6–3.0 M). From the c_{w50} values, it can be inferred that the concentrations of nerolidol that inhibit growth are approximately 5 to 6 times greater than those of miltefosine; however, the concentration of nerolidol that causes 50% hemolysis in PBS is approximately 100 times greater than that of miltefosine.

To estimate the membrane-plasma partition coefficient ($K_{M/P}$) for nerolidol in blood, we first estimated the erythrocyte membrane volume as $V_m = 1.05 \times 10^{-12}$ mL, assuming an average erythrocyte surface area of 135 μm^2 [33] and an erythrocyte membrane thickness of 78 Å [34]. This volume, V_m, is 85.7 times smaller than the average erythrocyte volume (90×10^{-12} mL). Because the concentration of

Table 1
Biophysical parameters associated with nerolidol interactions with the cell membranes of *L. amazonensis* amastigotes and promastigotes as well as J774.A1 macrophages and erythrocytes.

Cells	$K_{M/W}$ (10^4)[a]	log $K_{M/W}$	c_{w50} (μM)	c_{m50} (M)
Nerolidol				
Promastigotes	3.53 ± 0.56 (A)[b]	4.55	74 ± 6 (A)	2.6 ± 0.5 (A)
Amastigotes	5.35 ± 0.62 (B)	4.73	56 ± 4 (B)	3.0 ± 0.4 (A)
Macrophages	2.32 ± 0.26 (C)	4.37	125 ± 8 (C)	2.9 ± 0.4 (A)
Erythrocytes	0.13 ± 0.04 (D)	3.11	255 ± 38 (D)	0.3 ± 0.1 (B)
Comparison with miltefosine[c]				
Promastigotes	6.8	4.83	11	0.7
Amastigotes	14.4	5.16	12	1.7
Macrophages[d]	2.5	4.40	132	3.3
Erythrocytes	4.8	4.68	2.3	0.1

[a] The best-fit parameters were obtained using Eq. (6) and the data presented in Figs. 1, 2 and 3: $K_{M/W}$, membrane-water partition coefficient; c_{w50} and c_{m50}, nerolidol concentrations in the aqueous phase and the membrane that reduce the cell population by 50%, respectively.

[b] Statistical significance: in each column, the data with different capital letters are significantly different at $P < 0.05$.

[c] Data for miltefosine (means) reported in ref. [20] are shown for comparison.

[d] Peritoneal macrophages obtained from BALB/c mice.

nerolidol in aqueous medium is much lower than the concentration in the membrane ($K_{M/W}$ = 35,300, Table 1), we can neglect the amount of nerolidol inside the erythrocyte (also assuming that the volume of the inner membrane is small relative to that of the plasma membrane). Assuming a 42% hematocrit blood, the nerolidol concentration in plasma (c_{p50}) can be calculated as follows:

$$0.58\,(c_{p50}) + 0.42\left(\frac{c_{m50}}{85.7}\right) = HC_{50}. \quad (7)$$

Eq. (7) expresses that the HC_{50} value is given by the sum of the plasma fraction in blood (0.58) multiplied by the c_{p50} and the fraction of cells (0.42) multiplied by the average concentration of the molecule in the cell. Because the concentration of the molecule inside the cell was neglected, the average concentration in the cell was considered the membrane concentration (c_{m50}) diluted 85.7 times.

Because the c_{m50} was 300 mM (Table 1) and HC_{50} was 32 mM for nerolidol, the c_{p50} was 52.6 mM. Thus, the $K_{M/P}$ was equivalent to the c_{m50}/c_{p50} at 5.7 (assuming that the cell has an internal membrane volume three times larger than that of the plasma membrane, this calculation would result in $K_{M/P}$ = 6.7). A similar estimate for miltefosine produce a value of $K_{M/P}$ of 59 [22], indicating that in the blood, the affinity of nerolidol for the erythrocyte membrane is much less than that of miltefosine.

3.4. EPR spectroscopy

High cell concentrations are necessary to obtain good spectra in spin-label EPR experiments. Generally, 50 μL samples containing 1×10^8 cells are used, which corresponds to 2×10^9 cells/mL. Based on the c_{w50} and $K_{M/W}$ values shown in Table 1 for amastigotes, the corresponding nerolidol IC_{50} calculated for this cell concentration (using Eq. (6)) would be 1.84 mM.

To determine whether spin-label EPR spectroscopy could detect the changes caused by nerolidol in the plasma membrane of amastigotes at concentrations as low as those generally used in cell culture, we performed EPR experiments with a low concentration of cells in the suspension (4×10^7 cells/mL) but with a large volume (2 mL) to subsequently concentrate the cells enough to measure. Samples treated with different concentrations of nerolidol and after 2-h incubation at 32 °C were centrifuged to increase the cell concentration by 40 fold. The resulting EPR spectra are shown in Fig. 6 and indicate that 60 μM

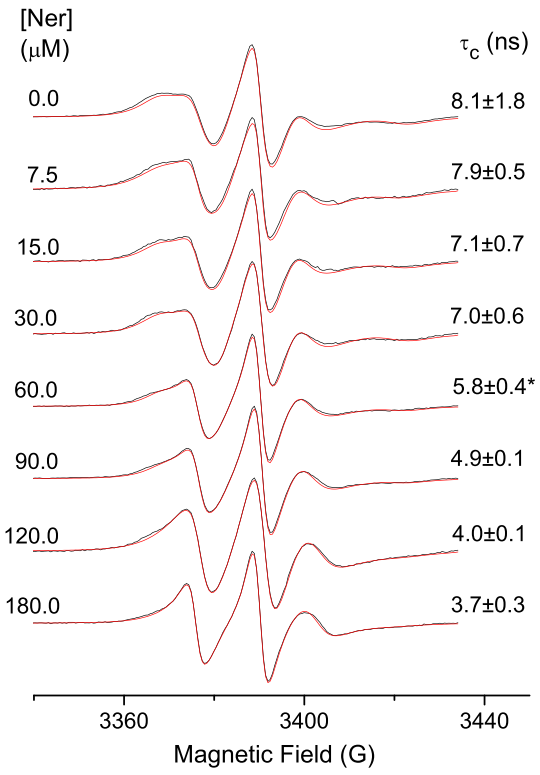

Fig. 6. Experimental (black line) and best-fit (red line) EPR spectra of 5-DSA in the plasma membrane of *Leishmania* amastigotes with and without treatment with several nerolidol concentrations. The best-fit spectra were obtained using a NLLS fit with a model of two spectral components. The values of the EPR parameter rotational correlation time (τ_c) obtained from the fits are indicated. *P < 0.05 compared to the control.

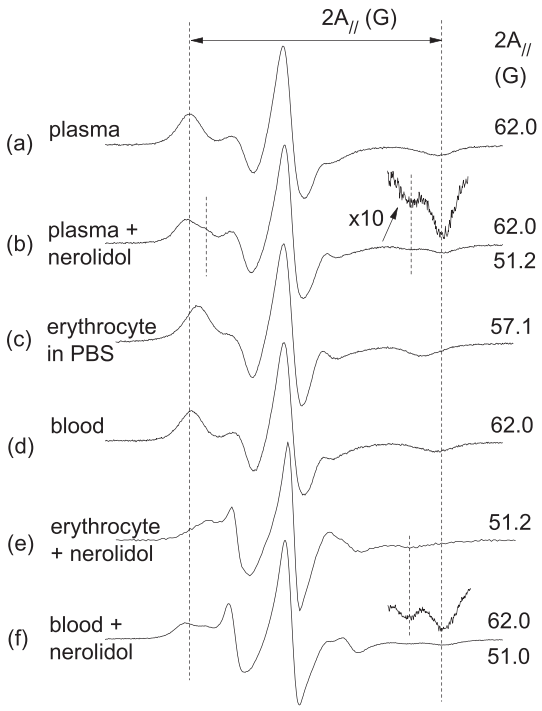

Fig. 7. EPR spectra of 5-DSA in plasma (a), plasma treated with 30 mM nerolidol (b), erythrocytes in PBS (c), whole blood (d), erythrocytes in PBS treated with 2 mM nerolidol (e) and blood treated with 30 mM nerolidol (f). The values of the EPR parameter $2A_{//}$ (outer hyperfine splitting), which is determined by the separation in magnetic field units between the first peak and the last inverted peak of the spectrum, are also indicated. For the spectra in (b) and (f), the values of the two resolved spectral components are indicated. The estimated experimental error for the $2A_{//}$ parameter is 0.5 G.

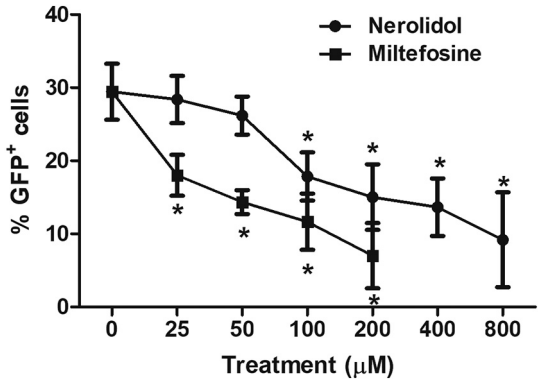

Fig. 8. Leishmanicidal action of nerolidol on *L. amazonensis*-infected J774.A1 macrophages. Percentage of cells expressing GFP compared to the untreated control was analyzed on a flow cytometer. *P < 0.05 compared to the control.

nerolidol is sufficient to increase the parasite membrane fluidity.

To compare the nerolidol effects on erythrocyte membranes of cells suspended in PBS and whole blood, we performed several EPR experiments using the spin-label 5-DSA (Fig. 7). The spectrum of 5-DSA in plasma (Fig. 7a) is characteristic of a spin label bound to serum albumin having an EPR $2A_{//}$ parameter of 62.0 G, similar to the case of BSA [35]. When plasma was treated with 30 mM nerolidol, the spectrum (Fig. 7b) showed two components, one indicating that most of the albumin remained unchanged ($2A_{//}$ = 62.0 G) and another corresponding to a small fraction of albumin with much greater dynamics ($2A_{//}$ = 51.2 G) due to the interaction with nerolidol. The spectrum of the spin-labeled erythrocyte membrane (Fig. 7c) indicated much greater molecular dynamics ($2A_{//}$ = 57.1 G) than that of plasma. In blood, every spin label seemed to be incorporated into albumin, and the spin-labeled spectral component in the erythrocyte membrane was not resolved in the spectrum (Fig. 7d). The spin-label EPR spectrum in erythrocyte membranes treated with nerolidol at 1× HC_{50} in PBS is shown in Fig. 7e, and this spectrum showed that the erythrocyte membrane became much more fluid at the nerolidol concentration that causes 50% hemolysis [15]. Fig. 7f shows the spectrum of the spin label in blood treated with 30 mM nerolidol (50% hemolysis in whole blood, Fig. 5) and indicates that the spin labels were distributed between the albumin ($2A_{//}$ = 62.0 G) and the erythrocyte membrane altered by nerolidol ($2A_{//}$ = 51.0 G).

3.5. Effect of nerolidol against intracellular amastigotes

To assess whether nerolidol controlled *L. amazonensis* infection in J774.A1 macrophages, we infected the cells with GFP-transfected *L. amazonensis* for 3 h and treated the cells with different concentrations of nerolidol for an additional 24 h for flow cytometry analysis. Miltefosine was used as a positive control. Nerolidol was able to significantly reduce the percentage of GFP positive cells at concentrations starting at 100 μM. Miltefosine succeeded in reducing the infection rate at lower concentrations compared to nerolidol (Fig. 8).

4. Discussion

In a previous study, spin-label EPR spectroscopy was used to examine the effects of the terpenes nerolidol, (+)-limonene, α-terpineol and 1,8-cineole on the plasma membrane of *L.* (*L.*) *amazonensis* promastigotes, and the results showed that the four terpenes increased the molecular dynamics of the parasite membrane and the concentration at which this effect was observed for each terpene was correlated with the

IC_{50} values of the terpenes [19]. Nerolidol was the most potent among the studied terpenes and exhibited an IC_{50} of 1.1 mM for 2×10^9 parasites/mL and a membrane effect at this concentration [19]. Compared with miltefosine, which can bind in large amounts to *Leishmania* membrane proteins and dramatically increase their molecular dynamics [20], nerolidol affects the lipid component of the membrane rather than the proteins. This effect was demonstrated using EPR spectroscopy with a spin label derived from maleimide (6-MSL) covalently bound to the sulfhydryl groups of *L.* (*L.*) *amazonensis* membrane proteins, and the EPR spectra indicated that miltefosine causes strong increases in the molecular dynamics of polypeptide chains while nerolidol causes only small changes at concentrations well above its IC_{50} [20,24]. In this study, EPR spectroscopy using a fatty acid spin label (5-DSA) demonstrated that nerolidol affects the membrane of *L. amazonensis* amastigotes and this effect could be detected with low concentrations of nerolidol (60 μM) if cell concentrations as low as 4×10^7 cells/mL were used in the experiment.

The affinity of nerolidol for the erythrocyte membrane was much lower than that for *Leishmania* and macrophages as deduced from the $K_{M/W}$ values (Table 1), and this pattern differs from that of miltefosine, which did not demonstrate large affinity differences for the three cell membranes. Thus, the c_{w50} for nerolidol was more than three-fold higher in erythrocytes than in *Leishmania*, while the inverse was observed in the case of miltefosine, for which the c_{w50} was approximately four-fold lower in erythrocytes. One disadvantage of nerolidol over miltefosine is that the difference between the IC_{50} values in *Leishmania* and CC_{50} in macrophages is lower for nerolidol (Table 1). While the concentration in the aqueous phase that inhibits parasite growth is in the micromolar range, the c_{m50} values of nerolidol in *Leishmania* were between 2.6 and 3.0 M, whereas the c_{m50} values of miltefosine were between 0.7 and 1.7 M. These data indicating such high drug membrane concentrations show the ability of these two compounds to accumulate in the plasma membrane of the parasite.

Importantly, in PBS, the HC_{50} valued ranged from 0.255 mM for samples with a low erythrocyte concentration (Table 1) to 2 mM to a 42% hematocrit (Fig. 3), whereas in whole blood (42% hematocrit), the HC_{50} was 32 mM, *i.e.*, 16-fold greater than the value in PBS. This result indicates that albumin in the blood sequesters an appreciable percentage of nerolidol. For a 42% hematocrit, the spin-label EPR data indicated that the nerolidol-induced changes in the erythrocyte membrane were similar to the changes in PBS and blood but occurred at nerolidol concentrations corresponding to the HC_{50} values in PBS (2 mM) and whole blood (32 mM). In blood, we considered that the nerolidol c_{m50} was 300 mM, which is equivalent to that estimated for PBS (Table 1). This assumption seems reasonable because the values are consistent with the membrane nerolidol changes indicated by the EPR spectra. With this assumption, the membrane-plasma partition coefficient (K_{MP}) for nerolidol in blood was estimated to be $K_{MP} = 5.7$, which is approximately ten times smaller than that for miltefosine [22]. Additionally, the measured nerolidol HC_{50} value in blood was approximately twenty times greater than that of miltefosine [22].

The effect of nerolidol against intracellular amastigotes was demonstrated in cultures of J774.A1 macrophages infected with GFP-transfected *L. amazonensis* from 100 μM of nerolidol after 24 h of treatment. Previous work has shown that the inhibition of intracellular amastigote growth assessed by counting the number of infected cells in monolayers of macrophages after 48 h of treatment was 85, 91 and 95% for nerolidol concentrations of 50, 75, and 100 μM, respectively [9]. This difference can be explained by the use of high-sensitivity flow cytometry in our study and the shorter treatment time. Although the transformation of promastigotes into amastigotes is a complex process that lasts > 24 h [36], long-term infections with cell lines such as J774.A1 are difficult to analyze because of the rapid proliferation of these cells. However, the internalization of most parasites occurs over a short time usually between 30 and 60 min [37]. Nevertheless, our data demonstrate that nerolidol is capable of interfering with parasites already internalized by macrophages. In this work, axenic *Leishmania* amastigotes were generated in a large quantity, and they presented a uniform population, which can facilitate comparisons with experiments with extracellular and intracellular amastigotes. The axenic *Leishmania* amastigote has been characterized, and the amastigote phenotype of most parasites is acquired based on light microscopy. However, only certain biological and biochemical properties of these axenic amastigote forms were experimentally analyzed [38].

A previous work [19] showed that the terpenes nerolidol, (+)-limonene, α-terpineol and 1,8-cineole at concentrations close to their IC_{50} values caused cell lysis of 4 to 9%, and all of these results are consistent with nerolidol attacking the plasma membrane of the parasite. It is important to consider that cell lysis may reduce the cell size and that the consequent electrolyte leakage affects the mitochondrial membrane potential. A cell membrane attack-based mode of action for nerolidol is consistent with its broad spectrum of activity *in vitro* [3]. For instance, nerolidol activity against *Schistosoma mansoni* adult worms has been demonstrated *in vitro*, and confocal laser scanning microscopy revealed morphological alterations in the tegument of worms, such as disintegration, sloughing and erosion of the surface [39]. A 24 h treatment of *L.* (*V.*) *braziliensis* promastigotes with nerolidol at the IC_{50} value has been shown to decrease cell size and mitochondrial membrane depolarization to an extent similar to that attained by treatment with amphotericin B at 2× IC_{50} [23]. Because nerolidol is a small and highly hydrophobic molecule and only has hydroxyl as a polar group, it exhibits rapid penetration and distribution throughout the cell membrane. In contrast, miltefosine contains the transporter LdMT and its beta subunit LdRos3, which facilitates the intake of this drug into the intracellular space of the parasite [40]. Our measurements were based on antiproliferative assays in which the miltefosine transporter was in its active form; thus, any interference from the transporter was considered in the calculations of the reported parameters. According to The Good Scents Company Information System, the Threshold of Concern for nerolidol is 1.8 mg/person/day [41]. Assuming an intake of nerolidol corresponding to the Threshold of Concern for a person with 5 L of blood as well as no loss of nerolidol, this amount would correspond to a nerolidol concentration of 1.6 μM in the blood. This concentration is well below the nerolidol IC_{50} value against leishmania identified *in vitro*. Because nerolidol accumulates in the cell membrane in large amounts, the daily intake of nerolidol could lead to its accumulation in the membranes of cells. However, due to this daily intake limit, it would take a relatively long time before the nerolidol level reaches a level that would show activity against leishmaniasis. However, nerolidol can be incorporated into an appropriately designed carrier, and this incorporation could increase the delivery of this agent to the target cells and potentiate its effectiveness.

5. Conclusions

Nerolidol showed a c_{w50} of 125 μM for J774.A1 macrophages, which was similar to that reported for miltefosine and peritoneal macrophages, although the nerolidol mean c_{w50} values of 56 μM for amastigotes and 74 μM for promastigotes of *L. amazonensis* were approximately 5-fold higher than that for miltefosine. The hemolytic potential of nerolidol in whole blood (HC_{50} = 32 mM) was lower than that reported for miltefosine (HC_{50} = 2.4 mM); and in PBS, we found c_{w50} values of 255 and 2.3 μM for nerolidol and miltefosine, respectively. The latter result was explained by a lower affinity of nerolidol for the erythrocyte membrane ($K_{M/W}$) and higher concentration required for membrane rupture (c_{m50}) in relation to miltefosine. In addition, the estimated values of nerolidol for the amastigotes and promastigotes of *L. amazonensis* and macrophages were between 2.6 and 3.0 M, indicating an important accumulation in the cell membrane. Spin-label EPR data indicated considerable increases in the molecular dynamics of the amastigote plasma membrane at concentrations similar to the nerolidol IC_{50} value. Taken together, these *in vitro* results suggest that the

first attack of nerolidol occurs at the parasite membrane.

Conflict of interest statement

The authors declare no conflicts of interest.

Transparency document

The Transparency document associated this article can be found, in online version.

Acknowledgments

This study was financially supported by grants from the Brazilian research funding agencies CNPq (445666/2014-5), CAPES and FAPEG (201210267001110). Lais Alonso is a recipient of a postdoctoral fellowship from CNPq (150369/2018-2). Antonio Alonso received a research grant from CNPq (303829/2016-8).

References

[1] World Health Organization, Leishmaniasis 14 March 2018, World Health Organization, Geneva, Switzerland, 2018http://www.who.int/news-room/fact-sheets/detail/leishmaniasis.
[2] World Health Organization. 2010. Control of the leishmaniasis: report of a meeting of the WHO Expert Committee on the Control of Leishmaniases, Geneva, 22–26 March 2010. (WHO Technical Report Series; No. 949).
[3] Chan WK, Tan LT, Chan KG, Lee LH, Goh BH. Nerolidol: a sesquiterpene alcohol with multi-faceted pharmacological and biological activities. Molecules 21(5). pii: E529, 2016. doi: https://doi.org/10.3390/molecules21050529.
[4] J. Triana, J.L. Eiroa, M. Morales, F.J. Pérez, I. Brouard, M.T. Marrero, et al., A chemotaxonomic study of endemic species of genus Tanacetum fromthe Canary Islands, Phytochemistry 92 (2013) 87–104.
[5] B.F. Brehm-Stecher, E.A. Johnson, Sensitization of Staphylococcus aureus and Escherichia coli to antibiotics by the sesquiterpenoids nerolidol, farnesol, bisabolol, and apritone, Antimicrob. Agents Chemother. 47 (10) (2003) 3357–3360.
[6] M.J. Park, K.S. Gwak, I. Yang, K.W. Kim, E.B. Jeung, J.W. Chang, I.G. Choi, Effect of citral, eugenol, nerolidol and alpha-terpineol on the ultrastructural changes of Trichophyton mentagrophytes, Fitoterapia 80 (2009) 290–296.
[7] S. Johann, F.B. Oliveira, E.P. Siqueira, P.S. Cisalpino, C.A. Rosa, T.M. Alves, C.L. Zani, B.B. Cota, Activity of compounds isolated from Baccharis dracunculifolia D.C. (Asteraceae) against Paracoccidioide brasiliensis, Med. Mycol. (8) (2012) 843–851.
[8] S. Hoet, C. Stévigny, M.F. Hérent, J. Quetin-Leclercq, Antitrypanosomal compounds from the leaf essential oil of Strychnos spinosa, Planta Med. 5 (2006) 480–482.
[9] D. Arruda, F. D'Alexandri, A. Katzin, S. Uliana, Antileishmanial activity of the terpene Nerolidol, Antimicrob. Agents Chemother. 49 (2005) 1679–1687.
[10] H. Rodrigues Goulart, E. Kimura, V. Peres, A. Couto, F. Aquino Duarte, A. Katzin, Terpenes arrest parasite development and inhibit biosynthesis of isoprenoids in Plasmodium falciparum, Antimicrob. Agents Chemother. 48 (2004) 2502–2509.
[11] A.Y. Saito, A.A. Marin Rodriguez, D.S. Menchaca Vega, R.A.C. Sussmann, E.A. Kimura, A.M. Katzin, Antimalarial activity of the terpene nerolidol, Int. J. Antimicrob. Agents 48 (6) (2016) 641–646.
[12] M. AbouLaila, T. Sivakumar, N. Yokoyama, I. Igarashi, Inhibitory effect of terpene nerolidol on the growth of Babesia parasites, Parasitol. Int. 59 (2) (2010) 278–282.
[13] Mendanha SA, Marquezin CA, Ito AS, Alonso A. Effects of nerolidol and limonene on stratum corneum membranes: a probe EPR and fluorescence spectroscopy study. Int. J. Pharm. 30; 532(1), 547–554, 2017. doi: 10.1016/j.ijpharm.2017.09.046.
[14] L. Alonso, C.A. Marquezin, P.J. Gonçalves, A. Alonso, Transmittance and autofluorescence of neonatal rat stratum corneum: nerolidol increases the dynamics and partitioning of protoporphyrin IX into intercellular membranes, J. Fluoresc. 26 (2016) 709–717, https://doi.org/10.1007/s10895-015-1758-z.
[15] S.A. Mendanha, S.S. Moura, J.L.V. Anjos, M.C. Valadares, A. Alonso, Toxicity of terpenes on fibroblast cells compared to their hemolytic potential and increase in erythrocyte membrane fluidit, Toxicol. in Vitro 27 (2013) 323–329, https://doi.org/10.1016/j.tiv.2012.08.022.
[16] S.A. Mendanha, A. Alonso, Effects of terpenes on fluidity and lipid extraction in phospholipid membranes, Biophys. Chem. 198 (2015) 45–54, https://doi.org/10.1016/j.bpc.2015.02.001.
[17] A.F. El-Kattan, C.S. Asbill, N. Kim, B.B. Michniak, The effects of terpene enhancers on the percutaneous permeation of drugs with different lipophilicities, Int. J. Pharm. 215 (2001) 229–240.
[18] A. Nokhodchi, K. Sharabiani, M.R. Rashidi, T. Ghafourian, The effect of terpene concentrations on the skin penetration of diclofenac sodium, Int. J. Pharm. 335 (1–2) (2007) 97–105.
[19] H.S. Camargos, R.A. Moreira, S.A. Mendanha, K.S. Fernandes, M.L. Dorta, A. Alonso, Terpenes increase the lipid dynamics in the leishmania plasma membrane at concentrations similar to their IC50 values, PLoS One 9 (2014) e104429, , https://doi.org/10.1371/journal.pone.0104429.
[20] K.S. Fernandes, P.E. de Souza, M.L. Dorta, A. Alonso, The cytotoxic activity of miltefosine against Leishmania and macrophages is associated with dynamic changes in plasma membrane proteins, Biochim. Biophys. Acta 1859 (1) (2017) 1–9, https://doi.org/10.1016/j.bbamem.2016.10.008.
[21] T.P. Dorlo, M. Balasegaram, J.H. Beijnen, P.J. de Vries, Miltefosine: a review of its pharmacology and therapeutic efficacy in the treatment of leishmaniasis, J. Antimicrob. Chemother. 67 (2012) 2576–2597, https://doi.org/10.1093/jac/dks275.
[22] L. Alonso, A. Alonso, Hemolytic potential of miltefosine is dependent on cell concentration: implications for in vitro cell cytotoxicity assays and pharmacokinetic data, Biochim. Biophys. Acta 1858 (2016) 1160–1164, https://doi.org/10.1016/j.bbamem.2016.03.004.
[23] L.F. Ceole, M.D.G. Cardoso, M.J. Soares, Nerolidol, the main constituent of Piper aduncum essential oil, has anti-Leishmania braziliensis activity, Parasitology 144 (9) (2017) 1179–1190, https://doi.org/10.1017/S0031182017000452.
[24] R.A. Moreira, S.A. Mendanha, K.S. Fernandes, G.G. Matos, L. Alonso, M.L. Dorta, A. Alonso, Miltefosine increases lipid and protein dynamics in Leishmania amazonensis membranes at concentrations similar to those needed for cytotoxicity activity, Antimicrob. Agents Chemother. 58 (2014) 3021–3028, https://doi.org/10.1128/AAC.01332-13.
[25] M.C. Teixeira, R. de Jesus Santos, R.B. Sampaio, L. Pontes-de-Carvalho, W.L. dos-Santos, A simple and reproducible method to obtain large numbers of axenic amastigotes of different Leishmania species, Parasitol. Res. 88 (2002) 963–968, https://doi.org/10.1007/s00436-002-0695-3.
[26] N. Gupta, N. Goyal, A.K. Rastogi, In vitro cultivation and characterization of axenic amastigotes of Leishmania, Trends Parasitol. 17 (2001) 150–153, https://doi.org/10.1016/S1471-4922(00)01811-0.
[27] V.H. Hodgkinson, L. Soong, S.M. Duboise, D. McMahon-Pratt, Leishmania amazonensis: cultivation and characterization of axenic amastigote-like organisms, Exp. Parasitol. 83 (1996) 94–105, https://doi.org/10.1006/expr.1996.0053.
[28] Okuda K, Tong M, Dempsey B, Moore KJ, Gazzinelli RT, Silverman N. Leishmania amazonensis engages CD36 to drive parasitophorous vacuole maturation. PLoS Pathog. 9;12(6):e1005669, 2016. doi: https://doi.org/10.1371/journal.ppat.1005669.
[29] D.E. Budil, S. Lee, S. Saxena, J.H. Freed, Nonlinear-least-squares analysis of slow-motion EPR spectra in one and two dimensions using a modified Levenberg-Marquardt algorithm, J. Magn. Reson. 120 (155–189) (1996) 1996, https://doi.org/10.1006/jmra.1996.0113.
[30] S.A. Mendanha, J.L.V. Dos Anjos, L. Maione-Silva, H.C.B. Silva, E.M. Lima, A. Alonso, An EPR spin probe study of the interactions between PC liposomes and stratum corneum membranes, Int. J. Pharm. 545 (1–2) (2018) 93–100, https://doi.org/10.1016/j.ijpharm.2018.04.057.
[31] A. Alonso, J. Vasques da Silva, M. Tabak, Hydration effects on the protein dynamics in stratum corneum as evaluated by EPR spectroscopy, Biochim. Biophys. Acta 1646 (32–41) (2003) 2003, https://doi.org/10.1016/S1570-9639(02)00545-9.
[32] L. Alonso, S.A. Mendanha, C.A. Marquezin, M. Berardi, A.S. Ito, A.U. Acuña, A. Alonso, Interaction of miltefosine with intercellular membranes of stratum corneum and biomimetic lipid vesicles, Int. J. Pharm. 434 (2012) 391–398, https://doi.org/10.1016/j.ijpharm.2012.06.006.
[33] R.E. Waugh, M. Narla, C.W. Jackson, T.J. Mueller, T. Suzuki, G.L. Dale, Rheologic properties of senescent erythrocytes: loss of surface area and volume with red blood cell age, Blood 79 (1992) 1351–1358.
[34] N.H. El-Farra, P.D. Christofides, J.C. Liao, Analysis of nitric oxide consumption by erythrocytes in blood vessels using a distributed multicellular model, Ann. Biomed. Eng. 31 (2003) 294–309, https://doi.org/10.1114/1.1553454.
[35] E.L. Gelamo, R. Itri, A. Alonso, J.V. da Silva, M. Tabak, Small-angle X-ray scattering and electron paramagnetic resonance study of the interaction of bovine serum albumin with ionic surfactants, J. Colloid Interface Sci. 277 (2) (2004) 471–482, https://doi.org/10.1016/j.jcis.2004.04.065.
[36] C.R. Alves, S. Corte-Real, S.C. Bourguignon, C.S. Chaves, E.M. Saraiva, Leishmania amazonensis: early proteinase activities during promastigote-amastigotedifferentiation in vitro, Exp. Parasitol. 109 (1) (2005) 38–48.
[37] N. Courret, C. Fréhel, N. Gouhier, M. Pouchelet, E. Prina, P. Roux, J.C. Antoine, Biogenesis of Leishmania-harbouring parasitophorous vacuoles following phagocytosis of the metacyclic promastigote or amastigote stages of the parasites, J. Cell Sci. 115 (2002) 2303–2316 Pt 11.
[38] A. Debrabant, M.B. Joshi, P.F. Pimenta, D.M. Dwyer, Generation of Leishmania donovani axenic amastigotes: their growth and biological characteristics, Int. J. Parasitol. 34 (2) (2004) 205–217.
[39] M.P. Silva, G.L. Oliveira, R.B. de Carvalho, D.P. de Sousa, R.M. Freitas, P.L. Pinto, J. de Moraes, Antischistosomal activity of the terpene nerolidol, Molecules 19 (3) (2014) 3793–3803, https://doi.org/10.3390/molecules19033793.
[40] F.J. Pérez-Victoria, M.P. Sánchez-Cañete, K. Seifert, S.L. Croft, S. Sundar, S. Castanys, F. Gamarro, Mechanisms of experimental resistance of leishmania to miltefosine: implications for clinical use, Drug Resist. Updat. 9 (2006) 26–39, https://doi.org/10.1016/j.drup.2006.04.001.
[41] TGSC Information System, http://www.thegoodscentscompany.com/data/rw1009032.html (accessed 13.03.19).